Segmental Dynamics and Self-Concentration around Chain Ends in Miscible Blend of Poly(cyclohexyl methacrylate) and Poly(cyclohexyl acrylate) As Studied by the Spin-Label Technique

Yohei Miwa,[†] Takuya Tanabe,[†] Katsuhiro Yamamoto,[†] Yusuke Sugino,[†] Masato Sakaguchi,[‡] Masahiro Sakai,[§] and Shigetaka Shimada*,[†]

Department of Materials Science & Engineering, Nagoya Institute of Technology, Gokiso-cho, Showa-ku, Nagoya 466-8555, Japan; Nagoya Keizai University, 61 Uchikubo, Inuyama 484-8503, Japan; and Research Center for Molecular-Scale Nanoscience, Institute for Molecular Science, 38 Nishigo-Naka, Myodaiji, Okazaki 444-8585, Japan

Received August 19, 2004; Revised Manuscript Received September 10, 2004

ABSTRACT: Local segmental dynamics of poly(cyclohexyl methacrylate) (PCHMA) and poly(cyclohexyl acrylate) (PCHA) in their miscible blend was determined by the spin-label technique. The PCHMA and PCHA chains were labeled with nitroxide radicals at chain ends or inside sites, respectively. The temperature-dependent electron spin resonance (ESR) spectra of the spin-labels selectively reflected the segmental dynamics around the labeled sites. Specific chain dynamics of the PCHMA and PCHA components in the blend was separately detected even though a single glass transition was observed in calorimetric measurements.The Lodge−McLeish model (L−M model) on the basis of the self-concentration effect in the blend predicted well the individual chain dynamics detected by the spin-labeling. This agreement implies that the local length scale to influence the dynamics is comparable to the Kuhn length, l_k. The chain ends of the PCHA and PCHMA in the homopolymer bulk had higher mobility than those of the inside sites due to flexibility around chain ends. The PCHMA chain end had higher mobility than that of inside segments in the blend with any compositions. On the other hand, the mobility of the PCHA chain end was lower than that of the inside in the blend when the weight fraction of the PCHA was smaller than ca. 0.5. These experimental results were described well by the L−M model with the lower self-concentration around chain ends. The lower self-concentration around chain ends is considered to be caused by the discontinuity of repeat units at chain ends.

Introduction

The characteristic around chain ends is one of the interesting topics in polymer science. Chain ends often greatly affect physical properties of polymeric materials. For example, Ueberreiter and Kanig interpreted the molecular weight dependence of a glass transition temperature (T_g) of polystyrene (PS) by considering a polymer as a copolymer comprised of inside and mobile chain end units,[1] and a concentration of chain ends to the surface of polymeric materials is one of the causes of a depression of the T_g at the surface.[2] These results imply that the mobility of chain ends is higher than that of inside units. In fact, some experiments[3−9] and computational techniques[10,11] have reported that the mobility around chain ends is higher than that of inside segments. The ESR spin-label technique is advantageous to detect the particular dynamics of polymer chains. We reported that the higher mobility of chain ends of PS,[3] poly(methyl methacrylate) (PMMA),[4] poly(methyl acrylate) (PMA),[5] and PS-*block*-PMA[5] in the bulk. Recently, Faller estimated local mobility of oligomers of PS and polyisoprene (PI) in their miscible blend by a computer simulation.[10] The chain ends of the both components showed high mobility in the blend, and it was found that the concentration of the counter component around the chain ends was higher than that around the inside segments.

Recently, the viscoelastic properties of miscible polymer blends have been focused on by means of experimental,[12−25] theoretical,[26] and computational[10,27,28] approaches. The failure of the empirical time−temperature superposition principle in describing system dynamics and individual chain dynamics of components has been detected. The Lodge−McLeish model (L−M model) based on the "self-concentration" effect of components induced by a chain connectivity predicted well the average dynamics of components in miscible blends.[26]

In a miscible polymer blend of polymer A and B, the chain connectivity imposes that the local environment of a segment of polymer A is (on average) necessarily richer in polymer A compared to the bulk composition (ϕ). The effective local concentration (ϕ_{eff}) sensed by a polymer segment is thus given by

$$\phi_{eff} = \phi_s + (1 - \phi_s)\phi \quad (1)$$

Here, ϕ_s is the "self-concentration" of the considered polymer segment. Lodge and McLeish suggested the way of calculating ϕ_s.[26] Their idea is that the length scale relevant to the monomeric friction factor should be of the same order as the Kuhn length, l_k, which is defined to be $C_\infty l$. C_∞ is the characteristic ratio, and l is the length of the average backbone bond. In the L−M model, it is assumed that the relaxation of the Kuhn segment is influenced by the concentration of monomers within a volume $V = {l_k}^3$. The ϕ_s is calculated as the

[†] Nagoya Institute of Technology.
[‡] Nagoya Keizai University.
[§] Institute for Molecular Science.
* Corresponding author: e-mail shimada.shigetaka@nitech.ac.jp.

10.1021/ma048288q CCC: $27.50
Published on Web 10/22/2004

volume fraction occupied by the Kuhn length's worth of monomers inside V:

$$\phi_s = C_\infty M_0 / k\rho N_{av} V \quad (2)$$

where M_0 is the molar mass of the repeat unit, N_{av} is the Avogadro number, k is the number of backbone bonds per repeat unit, and ρ is the density. Haley et al. reported that the control volume V relevant to the dynamics of the components in the blend was nearly temperature-independent.[23] Recently, individual segmental dynamics of poly(cyclohexyl methacrylate) (PCHMA) and poly(cyclohexyl acrylate) (PCHA) in the blend was detected by the spin-label technique, and the individual chain dynamics was predicted well by the L−M model.[29] The PCHMA and PCHA are a compatible pair.[30]

To our knowledge, this is the first work on segmental dynamics around chain ends in miscible blends. The dynamics and the effective composition around chain ends in the blend are interesting subjects. In the present paper, the molecular dynamics around the chain ends of the PCHMA and PCHA components in the blend was determined by the spin-labeling, and the self-concentration effect around chain ends was estimated.

Experimental Section

Materials. Inhibitors in cyclohexyl methacrylate (CHMA, Extra Pure Reagent, Tokyo Chemical Co., Ltd.), cyclohexyl acrylate (CHA, Extra Pure Reagent, Kishida Chemical Co., Ltd.), *tert*-butyl methacrylate (*t*BMA, Extra Pure Reagent, Tokyo Chemical), and *tert*-butyl acrylate (*t*BA, Extra Pure Reagent, Tokyo Chemical) were adsorbed on activate aluminum oxide (particle size 2−4 mm, Kanto Chemical Co., Inc.) and removed. *N*,*N*,*N*′,*N*′,*N*″-Pentamethyldiethylenetriamine (PMDETA, 99%, Aldrich Chemical Co., Ltd.), methyl 2-bromopropionate (MBrP, 98%, Aldrich), 2-bromopropionic acid *tert*-butyl ester (2-BABE, 97%, Tokyo Chemical), CuBr (98%, Aldrich), 1,1,4,7,10,10-hexamethyltriethylenetetramine (HMTETA, 97%, Aldrich), methyl α-bromoisobutyrate (MBIB, 99%, Fluka Chemical Co., Ltd.), *tert*-butyl α-bromoisobutyrate (*t*BBIB, 99%, Fluka Chemical) CuCl (95%, Nacalai Tesque), ethylenediaminetetraacetic acid (EDTA, Guaranteed Reagent, Nacalai Tesque), NaOH (Guaranteed Reagent, Nacalai Tesque), distilled water (Specially Prepared Reagent, Nacalai Tesque), and 2,2,6,6-tetramethyl-4-aminopiperidine-1-oxyl (4-amino-TEMPO, 99%, Aldrich) were used as received. Tetrahydrofuran (THF, Extra Pure Reagent, Nacalai Tesque) were distilled under reduced pressure. Toluene, anisole, and methanol were obtained from Nacalai Tesque (Extra Pure Reagent) and used without further purification.

Sample Synthesis and Selective Spin-Labeling. Chain End of PCHMA (1 in Figure 1). CHMA was polymerized via the atom transfer radical polymerization (ATRP) technique with the CuCl/HMTETA complex and *t*BBIB as an initiator in anisole.[31,32] The polymerization was carried out in a vacuum condition at 353 K. As a result, PCHMA which had a *tert*-butyl moiety at the chain end was prepared. The reaction mixture was dissolved into toluene and washed with water solution of EDTA/2Na (2 wt %) to remove the copper. For spin-labeling, an amide−ester interchange reaction between the *tert*-butyl moiety at the chain end and 4-amino-TEMPO was carried out in toluene at 283 K for 4 days. The spin-labeled PCHMA was precipitated from toluene solution to excess methanol and filtered to remove the large amount of unreacted spin-label reagents and dried in a vacuum at 363 K for 24 h. This precipitation was repeated more than four times to completely remove the unreacted spin-label reagents. The chemical structures of the spin-labeled PCHMA and PCHA are shown in Figure 1. The number-averaged molecular weight (M_n) and its distribution (M_w/M_n) of the all samples were determined by gel permeation chromatography (GPC) using PS standards (Tosoh). The M_n's and M_w/M_n's of the PCHMA and PCHA are listed in Table 1.

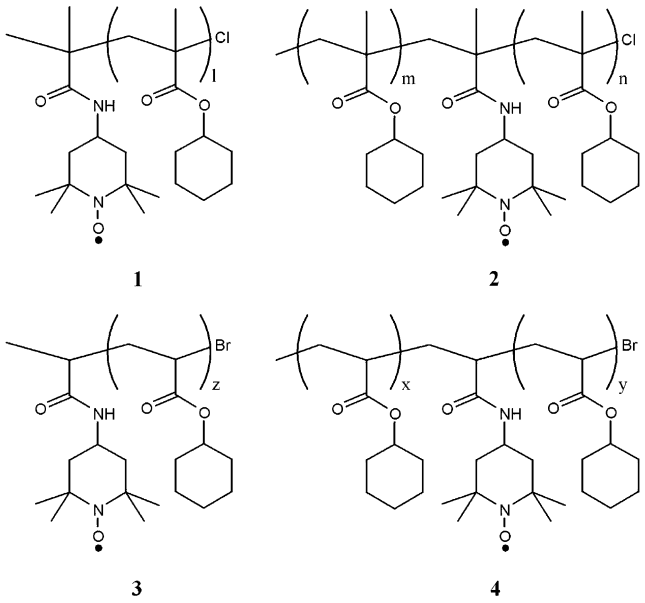

Figure 1. Chemical structures of PCHMA spin-labeled at chain end, **1**, and inside sites, **2**, and PCHA spin-labeled at chain end, **3**, and inside sites, **4**.

Table 1. Molecular Characteristics and T_{5mT}'s of PCHMA and PCHA

no.	polymer	spin-label site	M_n ($\times 10^3$)[a]	M_w/M_n[a]	T_{5mT} (K)[b]
1	PCHMA	chain end	11.5	1.18	434
2		inside	11.3	1.14	441
3	PCHA	chain end	15.1	1.13	373
4		inside	14.9	1.15	375

[a] Determined by GPC with PS standards. [b] Determined by ESR.

Inside Sites of PCHMA (2 in Figure 1). Poly(CHMA-*random*-*t*BMA) was polymerized by the ATRP with the CuCl/HMTETA and MBIB as an initiator. The initial molar compositions of *t*BMA was 1 mol % against the CHMA. The removal of the copper, the spin-labeling, and the purification of the sample were carried out with the same procedure described above.

Chain End of PCHA (3 in Figure 1). PCHA with a *tert*-butyl moiety at the α end was polymerized via the ATRP with the CuBr/PMDETA complex and 2-BABE as an initiator in anisole. The polymerization was carried out at 368 K.

Inside Sites of PCHA (4 in Figure 1). Poly(CHA-*random*-*t*BA) was polymerized by the ATRP with the CuBr/PMDETA and MBrP as an initiator at 368 K. The initial molar compositions of *t*BA was 1 mol % against the CHA.

Preparation of Blend Samples. PCHMA/PCHA blend samples were prepared as follows. First, PCHMA and PCHA were dissolved in THF to make 10 wt % solution and mixed with each other. The mixed solution was dried on a Teflon plate at 313 K. After the films were dried for 2 days, the films were annealed in a vacuum at 413 K for 24 h.

Measurement. GPC was carried out with following condition: in THF (1 mL/min) at 313 K on four polystyrene gel columns (Tosoh TSK gel GMH (beads size is 7 μm), G4000H, G2000H, and G1000H (5 μm)) that were connected to a Tosoh CCPE (Tosoh) pump and an ERC-7522 RI refractive index detector (ERMA Inc.). The columns were calibrated against standard PS (Tosoh) samples.

Each sample was contained in a quartz tube, and the tube was depressurized to a pressure of 10^{-4} Torr and sealed before ESR measurement. ESR spectra at 77 K and higher temperatures were observed at low microwave power level to avoid power saturation and with 100 kHz fielded modulation using JEOL JES-FE3XG and JES-RE1XG spectrometers (X band)

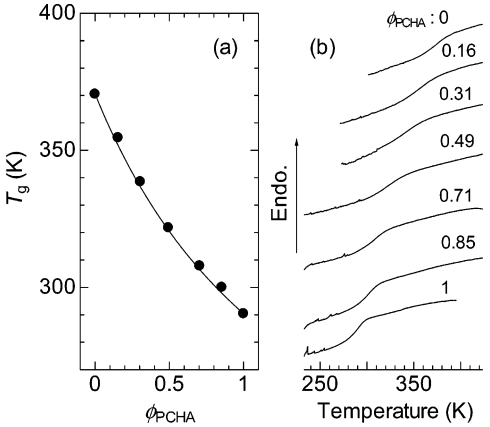

Figure 2. (a) Plots of T_g of PCHMA, PCHA, and blends as a function of ϕ_{PCHA}. Solid curve is presented by the Gordon−Taylor equation. (b) DSC traces.

coupled to microcomputers (NEC PC-9801). The signal of 1,1-diphenyl-2-picrylhydrazyl (DPPH) was used as a **g** tensor standard. The magnetic field was calibrated with the well-known splitting constants of Mn^{2+}.

Differential scanning calorimetry (DSC, MDSC 2920) manufactured by TA Instruments was used. Samples were heated from a room temperature to ca. T_g + 100 K at a rate of 20 K/min, kept for 5 min, and cooled at a rate of 10 K/min. The data collection was carried out on the cooling process. The calorimeter was calibrated with an indium standard.

Results and Discussion

1. DSC Measurements on PCHMA/PCHA Blend. DSC traces of the PCHMA/PCHA blends on the cooling process at a rate of 10 K/min are shown in Figure 2b. The PCHMA/PCHA blends with any compositions showed single glass transitions due to the compatible mixing of the both components. The T_g was taken to be the midpoint, i.e., the temperature corresponding to half of the endothermic shift. The T_g's of the PCHMA/PCHA blends were plotted against the weight fraction of the PCHA component (ϕ_{PCHA}) in Figure 2a. The T_g of the PCHMA/PCHA blend gradually decreased with an increase in the ϕ_{PCHA}, and the ϕ_{PCHA} dependence of the T_g was fitted well by the Gordon−Taylor relation[33] given by

$$T_g = (T_{g,PCHA}\phi_{PCHA} + KT_{g,PCHMA}(1 - \phi_{PCHA}))/(\phi_{PCHA} + K(1 - \phi_{PCHA})) \quad (3)$$

where $T_{g,PCHA}$ and $T_{g,PCHMA}$ are the glass transition temperatures of the PCHA and PCHMA homopolymers, respectively. K is a fitting parameter of 0.6.

2. Local Chain Dynamics Estimated by the Spin-Label Technique. 2.1. High Mobility around Chain Ends in PCHMA and PCHA Homopolymers. Temperature-dependent ESR spectra of the spin-labeled PCHMA and PCHA homopolymers are shown in the range 77−450 K (Figure 3). Both of the PCHMA and PCHA were spin-labeled at the chain end or inside sites, respectively. The temperature dependence of the spectra is brought from changes of the τ_c of the spin-labels. The nitroxides (spin-labels) show the triplet spectrum due to the hyperfine coupling of the nitrogen nucleus, and the outermost splitting width of the triplet spectrum narrows with an increase in mobility of the nitroxides because of motional averaging of the anisotropic interaction between the electron and the nucleus. The complete averaging gives rise to the isotropic narrowed spectrum.[34]

The extreme separation widths between arrows in Figure 3 are plotted against temperature in Figure 4. The extreme separation width gradually decreases and steeply drops with the increase in temperature. T_{5mT} at which the extreme separation width is equal to 5.0 mT is estimated as a transition temperature of the molecular motion. The T_{5mT}'s of the PCHA labeled at the chain end ($T_{5mT,e,1}$) and inside sites ($T_{5mT,i,1}$) are 373 and 375 K, respectively. Similarly, those of the PCHMA labeled at the chain end ($T_{5mT,e,2}$) and inside sites ($T_{5mT,i,2}$) are 434 and 441 K, respectively. Note that the difference between the $T_{5mT,e,1}$ and $T_{5mT,i,1}$ was small. Therefore, the reproducibility of the experimental result is very important on this work. Then the ESR measurements were carried out several times for each sample, and the same ESR spectra were obtained. Anyhow, the higher molecular mobility of chain ends than that of inside sites was concluded for both of the PCHMA and PCHA homopolymers by the analysis of the temperature-dependent ESR spectra. Recently, we detected high mobility around chain ends of PS, PMA, and PMMA by the spin-label method.[3−5] The molecular weight dependence of the mobility of the chain ends was observed as well as the T_g. We concluded that the mobility of spin-labels at chain ends reflected the α relaxation around chain ends because local motions (β and γ) might demonstrate no molecular weight dependence. Anyhow, the high mobility around chain ends is considered to be brought from flexibility around chain ends. Some computational results[10,11] also supported the higher mobility around chain ends in the bulk.

The T_{5mT} appears at higher temperature than the T_g of the samples determined by the DSC because of a high frequency of the ESR (X-band).[35−37] Recently, we estimated the difference between the T_{5mT} and T_g of PCHMA, PCHA, polystyrene (PS), and poly(methyl methacrylate) (PMMA) using the time−temperature superposition (the WLF equation),[3,4,29] and it was found that the T_{5mT} reflected the glass transition of the host polymers at the frequency of the ESR.

2.2. Each Segmental Dynamics of PCHMA and PCHA Components in the Blend. The "spin-labeled PCHMA (chain end or inside)"/PCHA and PCHMA/"spin-labeled PCHA (chain end or inside)" blends with the same composition were prepared to determine the local segmental dynamics of the spin-labeled sites in the blend by the ESR. The temperature-dependent ESR spectra selectively reflect the mobility of the spin-labeled sites in the blend. Temperature-dependent ESR spectra of the PCHMA and PCHA labeled at chain ends and inside sites in the blends with ϕ_{PCHA} = 0.25 were compared in Figure 5. All spin-labeled sites showed different segmental dynamics even though the both components were compatibly mixing. The T_{5mT} of the PCHMA labeled at the chain end ($T_{5mT,e,PCHMA}$) and inside sites ($T_{5mT,i,PCHMA}$) in the blend were 420 and 424 K, respectively, and those of the PCHA labeled at the chain end ($T_{5mT,e,PCHA}$) and inside sites ($T_{5mT,i,PCHA}$) in the blend were 412 and 410 K, respectively. Recently, we showed that the individual chain dynamics of the PCHMA and PCHA components detected by the ESR in the blend were affected by the difference of the local composition around the labels.[29] Features of the dynamics of the both components were interpreted well by the L−M model.[26]

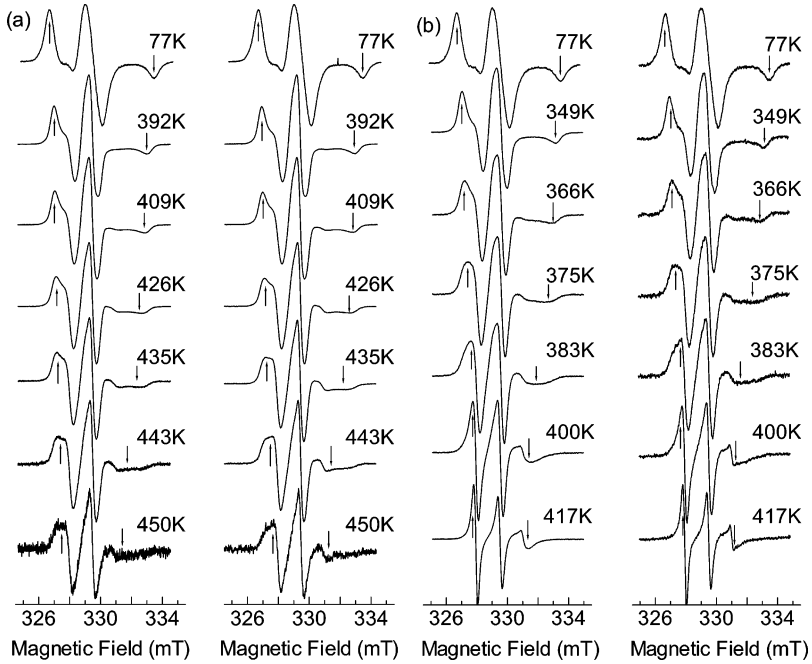

Figure 3. Temperature-dependent ESR spectra of PCHMA labeled at inside (left in (a)) and chain end (right in (a)) and those of PCHA labeled at inside (left in (b)) and chain end (right in (b)). Separation between arrows shows extreme separation width.

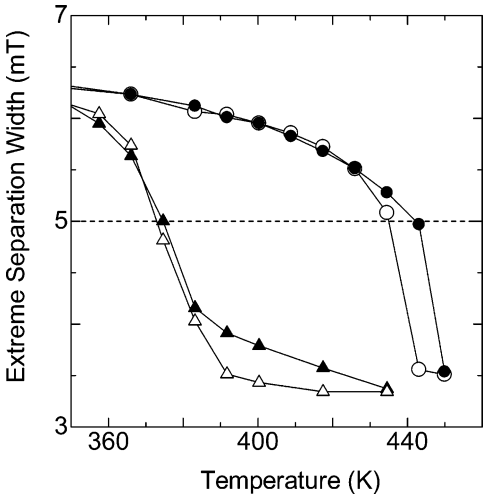

Figure 4. Temperature dependence of extreme separation widths of PCHMA labeled at inside (solid circle) and chain end (open circle), and that of PCHA labeled at inside (solid triangle) and chain end (open triangle) shown in Figure 3.

The chain end of the PCHMA had higher mobility than that of the inside sites in the blend with the ϕ_{PCHA} of 0.25 as well as in the homopolymer. On the other hand, it is interesting that the chain end of the PCHA showed lower mobility than that of the inside sites in the blend. These are very instructive results to discuss the self-concentration effect around chain ends in the blend. Previously, we reported that a cooperative motion between chain ends and inside segments was necessary for PS and PMMA chain ends to undergo a rotational relaxation,[3,4] and the blending with the PCHMA obviously depressed the mobility of the PCHA chain end. This demonstrates the cooperativity between the PCHA chain end and the PCHMA segments. The self-concentration effect around the chain ends in the blend was estimated in the following section.

2.3. Effective T_{5mT} Evaluated by the L−M Model. As reported previously, it is considered that the spin-labels are meshed with neighboring monomeric units in the bulk, and as a result, they move cooperatively with the neighboring monomeric units.[3,4,29] The mobility of spin-labels was strongly influenced by the composition around the labels in the blend.[29] Recently, we showed that the $T_{5mT,i,PCHMA}$ and $T_{5mT,i,PCHA}$ were predicted well by the L−M model which took into account the effective local concentration, ϕ_{eff}, around the labels. In the previous work, we evaluated the self-concentration, ϕ_s, of the PCHMA and PCHA to be ca. 0.41 and 0.21, respectively.[29] It was assumed that the "effective" motional transition temperature, T^{eff}_{5mT}, is as follows

$$T^{eff}_{5mT}(\phi) = T_{5mT}(\phi)|_{\phi=\phi_{eff}} \quad (4)$$

where $T_{5mT}(\phi)$ corresponds to the motional transition temperature of the blend of average concentration, ϕ. We calculated the evolution of the T^{eff}_{5mT} of the PCHMA and PCHA following the same procedure as Lodge and McLeish, i.e., by combining eqs 1, 3, and 4. For example, the T^{eff}_{5mT} of the PCHA labeled at the inside ($T^{eff}_{5mT,i,PCHA}$) is given by

$$T^{eff}_{5mT,i,PCHA} = (T_{5mT,i,1}\phi_{eff,PCHA} + KT_{5mT,i,2}(1 - \phi_{eff,PCHA}))/(\phi_{eff,PCHA} + K(1 - \phi_{eff,PCHA})) \quad (5)$$

The $\phi_{eff,PCHA}$ is the effective concentration of the PCHA component calculated by eq 1. Here, K was substituted to be 0.6 from the DSC result.

The $T^{eff}_{5mT,i,PCHMA}$ and $T^{eff}_{5mT,i,PCHA}$ predicted by the L−M model are presented as solid curves in parts a and b of Figure 6, respectively. The $T^{eff}_{5mT,i,PCHMA}$ was in excellent agreement with the experimental $T_{5mT,i,PCHMA}$ as well as our previous work.[29] This result implies that the volume to influence to the dynamics of the spin-labels is comparable to the l_k^3 proposed by Lodge and McLeish. As mentioned above, the T_{5mT} is higher than the T_g determined by the DSC due to the high frequency of the ESR. Haley et al. showed that the control volume V relevant to the dynamics of the components in the blend was nearly temperature-independent.[23] Our

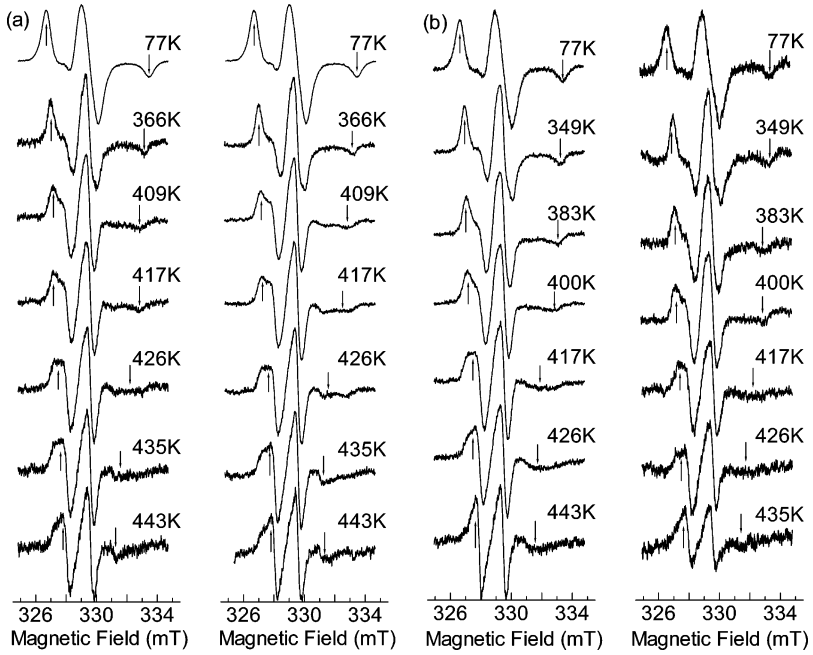

Figure 5. Temperature-dependent ESR spectra of (a) PCHMA labeled at inside (left) and chain end (right) and (b) PCHA labeled at inside (left) and chain end (right) in the blend with $\phi_{PCHA} = 0.25$.

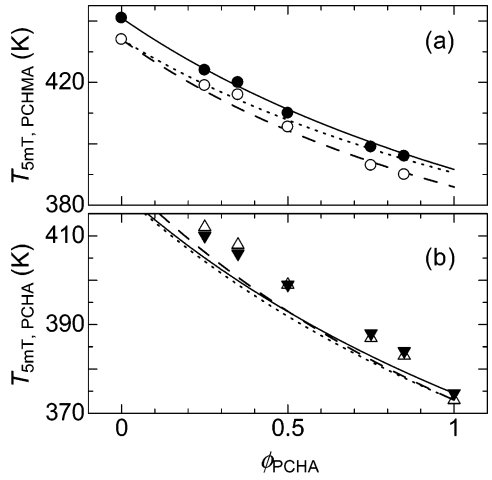

Figure 6. (a) Plots of $T_{5mT,i,PCHMA}$ (solid) and $T_{5mT,e,PCHMA}$ (open) against ϕ_{PCHA}. Solid curve is $T^{eff}_{5mT,i,PCHMA}$ with ϕ_s of 0.41. Broken and dotted curves are $T^{eff}_{5mT,e,PCHMA}$'s calculated with ϕ_s of 0.30 and 0.41, respectively. (b) Plots of $T_{5mT,i,PCHA}$ (solid) and $T_{5mT,e,PCHA}$ (open) against ϕ_{PCHA}. Solid curve is $T^{eff}_{5mT,i,PCHA}$ with ϕ_s of 0.21. Broken and dotted curves are $T^{eff}_{5mT,e,PCHA}$'s calculated with ϕ_s of 0.15 and 0.21, respectively.

result supports their result. On the other hand, the experimental $T_{5mT,i,PCHA}$ was slightly higher than the $T^{eff}_{5mT,i,PCHA}$ predicted by the L−M model, but the L−M model qualitatively interpreted the feature of the $T_{5mT,i,PCHA}$ nevertheless. One of the causes of this disagreement might be related to the ambiguous parameters used to calculate the ϕ_s and the simplification of the L−M model. As reported previously, mobility of the poly(acrylate)s in multicomponents system tends to be higher than the expected one, and understanding the causes of this behavior is important.[29] However, the reason is still unknown.

2.4. Self-Concentration around Chain Ends in the Blend. The mobility of the PCHMA chain ends was higher than that of the inside segments in the blend with any compositions. On the other hand, it is interesting that the $T_{5mT,e,PCHA}$ was higher than the $T_{5mT,i,PCHA}$ when the ϕ_{PCHA} was less than ca. 0.5. This implies that the mobility around the PCHA chain ends is lower than that of the inside segments in these compositions. These experimental $T_{5mT,e,PCHMA}$ and $T_{5mT,e,PCHA}$ were compared with T^{eff}_{5mT} of the PCHMA and PCHA labeled at the chain ends ($T^{eff}_{5mT,e,PCHMA}$ and $T^{eff}_{5mT,e,PCHA}$) calculated by the L−M model in parts a and b of Figure 6, respectively. For example, the $T^{eff}_{5mT,e,PCHA}$ was given by

$$T^{eff}_{5mT,e,PCHA} = (T_{5mT,e,1}\phi_{eff,PCHA} + KT_{5mT,i,2}(1 - \phi_{eff,PCHA}))/(\phi_{eff,PCHA} + K(1 - \phi_{eff,PCHA})) \quad (6)$$

where K was substituted to be 0.6.

The $T^{eff}_{5mT,e,PCHA}$ calculated with the ϕ_s of 0.21 was presented as a dotted curve in Figure 6b. Similarly, the $T^{eff}_{5mT,e,PCHMA}$ calculated with the ϕ_s of 0.41 was drawn in Figure 6a (dotted curve). The $T^{eff}_{5mT,e,PCHA}$ is smaller than the $T^{eff}_{5mT,i,PCHA}$ in any compositions (Figure 6b). However, the experimental $T_{5mT,e,PCHA}$ was higher than the $T_{5mT,i,PCHA}$ when the ϕ_{PCHA} was lower than ca. 0.5. For the PCHMA, the $T^{eff}_{5mT,e,PCHMA}$ (dotted curve) was somewhat higher than the $T_{5mT,e,PCHMA}$, and the difference was especially apparent in the case that the ϕ_{PCHA} was large (Figure 6a). These dotted curves were inappropriate to describe the experimental results. On the other hand, the $T^{eff}_{5mT,e,PCHMA}$ calculated with the ϕ_s of 0.3 fitted well the experimental $T_{5mT,e,PCHMA}$ (broken curve in Figure 6a). For the PCHA, the $T^{eff}_{5mT,e,PCHA}$ calculated with the ϕ_s of 0.15 (broken curve in Figure 6b) become higher than the $T^{eff}_{5mT,i,PCHA}$ when the ϕ_{PCHA} is less than ca. 0.5. The broken and solid curves captured the relationship between the $T_{5mT,i,PCHA}$ and $T_{5mT,e,PCHA}$, respectively. Note that this estimation is qualitative for the PCHA component because of the disagreement between the $T_{5mT,i,PCHMA}$ and the $T^{eff}_{5mT,i,PCHMA}$. However, these results obviously indicate that the smaller ϕ_s around chain ends than that for inside segments is necessary to interpret the experimental results by the L−M model. This implies that the

self-concentration effect is small around chain ends in the blend; namely, the effective composition around chain ends is closer to the average composition. In the L−M model, the decrease in the ϕ_s implies an increase in the V around the noticed spot. However, the lower self-concentration around chain ends is considered to be caused by the discontinuity of repeat units at the chain end. The discontinuity should decrease the concentration of the labeled component around the spin-labels. The higher $T_{5mT,e,PCHA}$ than the $T_{5mT,i,PCHA}$ is considered to be brought from the locally higher PCHMA composition around the PCHA chain ends than that around the inside segments in the blend. Recently, Faller estimated local segmental dynamics of oligomers (15-mers) of PS and PI in the miscible blend using a computer simulation.[10] It was concluded that the self-concentration around chain ends was lower than that around inside sites. Our experimental result supported his simulation result, and Faller reported that the fastest PI segments in the even blend were mostly chain ends. However, our result emphasizes that not all chain ends of a lower T_g component are the most mobile segment in the blend; it depends on the local composition around the chain ends.

Conclusion

The individual chain dynamics of the PCHMA and PCHA in the blend detected by the spin-labeling was interpreted by the L−M model. This agreement implies that the volume relative to the dynamics of the spin-labels is comparable to the l_k^3. Determination of mobility around chain ends in the blend was effective to evaluate the self-concentration around chain ends. Chain ends of the PCHMA and PCHA showed higher mobility than that of inside segments in the homopolymer bulk due to the flexibility around the chain ends. The mobility around the PCHMA chain ends was higher than that of inside segments in the blend with any compositions. On the other hand, the mobility of PCHA chain ends in the blend was lower than that of inside segments when the ϕ_{PCHA} was lower than ca. 0.5. The locally higher PCHMA composition around the PCHA chain ends was the cause of this behavior. These experimental results were described well by the L−M model with the smaller ϕ_s around chain ends. The smaller self-concentration effect around chain ends was considered to be brought from the discontinuity of repeat units at the chain ends. This experimental result is in good agreement with the computational anticipation reported by Faller. In conclusion, the discontinuity of the repeat units at chain ends brings the higher mobility and the lower self-concentration around chain ends in the blend.

Acknowledgment. This research was partially supported by the Ministry of Education, Science, Sports and Culture, Grant-in-Aid for Young Scientists (B), 16750185, 2004. Thanks are due to the Research Center for Molecular-Scale Nanoscience, the Institute for Molecular Science, for assistance in obtaining the DSC data.

References and Notes

(1) Ueberreiter, K.; Kanig, G. *J. Colloid Sci.* **1952**, *7*, 569.
(2) Tanaka, K.; Takahara, A.; Kajiyama, T. *Macromolecules* **2000**, *33*, 7588.
(3) Miwa, Y.; Tanase, T.; Yamamoto, K.; Sakaguchi, M.; Sakai, M.; Shimada, S. *Macromolecules* **2003**, *36*, 3235.
(4) Miwa, Y.; Yamamoto, K.; Sakaguchi, M.; Shimada, S. *Polym. Prepr.* **2004**, *45*, 792.
(5) Miwa, Y.; Yamamoto, K.; Sakaguchi, M.; Sakai, M.; Tanida, K.; Hara, S.; Okamoto, S.; Shimada, S. *Macromolecules* **2004**, *37*, 831.
(6) Waldow, D. A.; Ediger, M. D.; Yamaguchi, Y.; Matsushita, Y.; Noda, I. *Macromolecules* **1991**, *24*, 3147.
(7) Glowinkowski, S.; Gisser, D. J.; Ediger, M. D. *Macromolecules* **1990**, *23*, 3520.
(8) Adolf, D. B.; Ediger, M. D.; Kitano, T.; Ito, K. *Macromolecules* **1992**, *25*, 867.
(9) Horinaka, J.; Maruta, M.; Ito, S.; Yamamoto, M. *Macromolecules* **1999**, *32*, 1134.
(10) Faller, R. *Macromolecules* **2004**, *37*, 1095.
(11) Tokita, N.; Hirabayashi, M.; Azuma, C.; Dotera, T. *J. Chem. Phys.* **2004**, *120*, 496.
(12) Kant, R.; Kumar, S. K.; Colby, R. H. *Macromolecules* **2003**, *36*, 10087.
(13) Kumar, S. K.; Colby, R. H.; Anastasiadis, S. H.; Fytas, G. *J. Chem. Phys.* **1996**, *105*, 377.
(14) Leroy, E.; Alegria, A.; Colmenero, J. *Macromolecules* **2003**, *36*, 7280.
(15) Leroy, E.; Alegria, A.; Colmenero, J. *Macromolecules* **2002**, *35*, 5587.
(16) Colby, R. H. *Polymer* **1989**, *30*, 1275.
(17) Chung, G.-C.; Kornfield, J. A.; Smith, S. D. *Macromolecules* **1994**, *27*, 964.
(18) Chung, G.-C.; Kornfield, J. A.; Smith, S. D. *Macromolecules* **1994**, *27*, 5729.
(19) Alvarez, F.; Alegria, A.; Colmenero, J. *Macromolecules* **1997**, *30*, 597.
(20) Min, B.; Qiu, X.; Ediger, M. D.; Pitsikalis, M.; Hadjichristidis, N. *Macromolecules* **2001**, *34*, 4466.
(21) Zetsche, A.; Fischer, E. W. *Acta Polym.* **1994**, *45*, 168.
(22) Kamath, S.; Colby, R. H.; Kumar, S. K.; Karatasos, K.; Floudas, G.; Fytas, G.; Roovers, J. E. L. *J. Chem. Phys.* **1999**, *111*, 6121.
(23) Haley, C. J.; Lodge, P. T.; He, Y.; Ediger, M. D.; von Meerwall, E. D.; Mijovic, J. *Macromolecules* **2003**, *36*, 6142.
(24) Alegria, A.; Gomez, D.; Colmenero, J. *Macromolecules* **2002**, *35*, 2030.
(25) Hoffmann, S.; Willner, L.; Richter, D.; Arbe, A.; Colmenero, J.; Farago, B. *Phys. Rev. Lett.* **2000**, *85*, 772.
(26) Lodge, T. P.; McLeish, T. C. B. *Macromolecules* **2000**, *33*, 5278.
(27) Heine, D.; Wu, D. T.; Curro, J. G.; Grest, G. S. *J. Chem. Phys.* **2003**, *118*, 914.
(28) Salaniwal, S.; Kant, R.; Colby, R. H.; Kumar, S. K. *Macromolecules* **2002**, *35*, 9211.
(29) Miwa, Y.; Sugino, Y.; Yamamoto, K.; Tanabe, T.; Sakaguchi, M.; Sakai, M.; Shimada, S. *Macromolecules* **2004**, *37*, 6061.
(30) Siol, W.; GmbH, R. *Makromol. Chem., Macromol. Symp.* **1991**, *44*, 47.
(31) Patten, T. E.; Xia, J.; Abernathy, T.; Matyjaszewski, K. *Science* **1996**, *272*, 866.
(32) Matyjaszewski, K.; Patten, T. E.; Xia, J. *J. Am. Chem. Soc.* **1997**, *119*, 674.
(33) Gordon, M.; Taylor, S. J. *J. Appl. Chem.* **1952**, *2*, 4.
(34) Miwa, Y.; Tanida, K.; Yamamoto, K.; Okamoto, S.; Sakaguchi, M.; Sakai, M.; Makita, S.; Sakurai, S.; Shimada, S. *Macromolecules* **2004**, *37*, 3707.
(35) Shimada, S.; Kashima, K. *Polym. J.* **1996**, *28*, 690.
(36) Sohma, J.; Sakaguchi, M. *Adv. Polym. Sci.* **1978**, *20*, 109.
(37) Kusumoto, N.; Sano, S.; Zaitsu, N.; Motozato, Y. *Polymer* **1976**, *17*, 448.

MA048288Q